

# Effects of the Non-Proportional Loading Path on the Fatigue Crack Path

M. de Freitas, L. Reis, M. Leite and B. Li

Department of Mechanical Engineering, Instituto Superior Técnico, Av. Rovisco Pais, 1049-001 Lisboa, Portugal. E-mail: mfreitas@dem.ist.utl.pt

**ABSTRACT.** *Fatigue crack path prediction and crack arrest are very important for structural safety. In real engineering structures, there are many factors influencing the fatigue crack paths, such as the material type (microstructure), structural geometry and loading path, etc. This paper studies the effects of loading path on the crack path. Experiments were conducted on a biaxial testing machine, on the specimen made of steel 42CrMo4, with six different biaxial loading paths. Fractographical analyses of the plane of crack initiation and propagation were carried out. Theoretical predictions of the damage plane were conducted using the Findley, the Fatemi-Socie, the SWT and the Liu's criteria. Comparisons of the predicted orientation of the damage plane with the experimental observations show that the shear-based multiaxial fatigue models give very good predictions.*

## INTRODUCTION

In structural durability analyses, the prediction of the potential crack path as well as fatigue lifetime is very important for safety evaluations. In a critical component or structure, the crack path can determine whether fatigue failure is benign or catastrophic. Besides, the knowledge of potential crack paths is also important for the selection of appropriate non-destructive testing procedures and structural design for crack arrest. Therefore, the study on the crack paths has received increasing attentions in the recent years.

In real engineering structures, there are many factors influencing the fatigue crack paths, such as the material type (microstructure), structural geometry and loading path, etc. The objective of this paper is to study the effects of non-proportional loading paths on the fatigue crack paths. In the experimental studies, six loading cases are tested and the crack plane orientation are analysed by optical microscope.

The influence of the loading paths on the crack orientation was observed. Then the multiaxial fatigue models, such as the critical plane models and also the energy-based critical plane models, are applied for predicting the orientation of the critical plane. The predictions are compared with experimental and observations. The applicability of the multiaxial models is discussed for the material and loading paths studied.

## MATERIAL DATA, SPECIMEN FORM AND TEST PROCEDURES

The material studied in this paper is the high strength steel 42CrMo4. The chemical composition and monotonic mechanical properties are shown in Tables 1 and 2, respectively.

Table 1. Chemical composition of the material studied (in wt%).

	C	Si	Mn	P	S	Cr	Ni	Mo	Cu
42CrMo4	0.39	0.17	0.77	0.025	0.020	1.10	0.30	0.16	0.21

Table 2. Monotonic mechanical properties of the material studied.

Tensile strength	Ru (MPa)	1100
Yield strength	Rp0.2, monotonic (MPa)	980
Elongation	A (%)	16
Young's modulus	E (GPa)	206
Hardness	HV	362

The geometry and dimensions of the specimen are shown in Fig. 1.

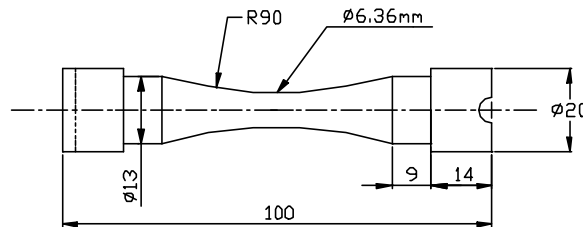


Figure 1. Specimen geometry for biaxial cyclic tension-compression with cyclic torsion tests.

In order to characterize the cyclic stress-strain behaviour of the materials studied, tension-compression low cycle fatigue tests were carried out using a biaxial servo-hydraulic machine. The cyclic properties obtained by fitting the test results are shown in Table 3.

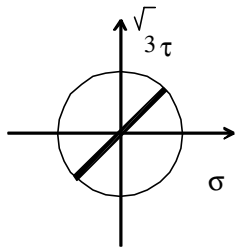
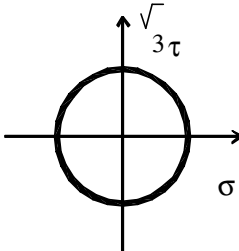
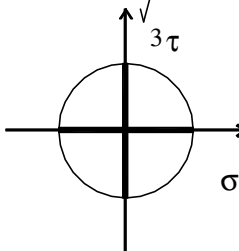
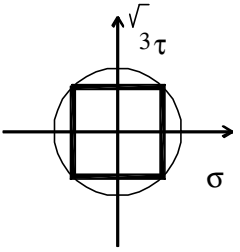
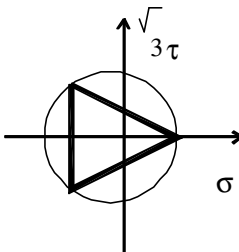
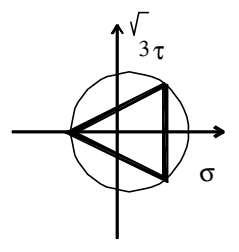
To study the effects of the loading paths on the fatigue crack paths, a series of loading paths were applied in the experiments as shown in Table 4. Tests of biaxial cyclic tension-compression with cyclic torsion were performed by a biaxial servo-hydraulic machine. Test conditions were as follows: frequency 4-6 Hz and room temperature in laboratory air. Tests ended up when the specimens were completely

broken. Following, fractographical analysis of the macroscopic plane of crack initiation and early crack growth were carried out, using an optical microscope at a magnification between 10 and 100 times. Some of the specimens were also analysed in the SEM microscope. The measurement of the crack initiation plane orientation was carried as follows: first, the crack initiation was identified, as shown in Fig. 2, left side, by an arrow; second, the specimen was analysed in a 3D measurement device and the angle between the crack initiation plane and the longitudinal axis was accurately measured, right side of Fig. 2. This procedure and some example for each loading path are shown in Fig. 2.

Table 3. Cyclic properties of the material studied ( $f=0.2s^{-1}$ ).

		42CrMo4
Yield strength	$R_{p,0.2,cyclic}$ (MPa)	650
Strength coefficient	$K'$ (MPa)	1420
Strain hardening exponent	$n'$	0.12
Fatigue strength coefficient	$\sigma'_f$ (MPa)	1154
Fatigue strength exponent	$b$	-0.061
Fatigue ductility coefficient	$\hat{a}_f'$	0.18
Fatigue ductility exponent	$c$	-0.53

Table 4. Multiaxial fatigue loading paths.

		
Case 1	Case 2	Case 3
		
Case 4	Case 5	Case 6

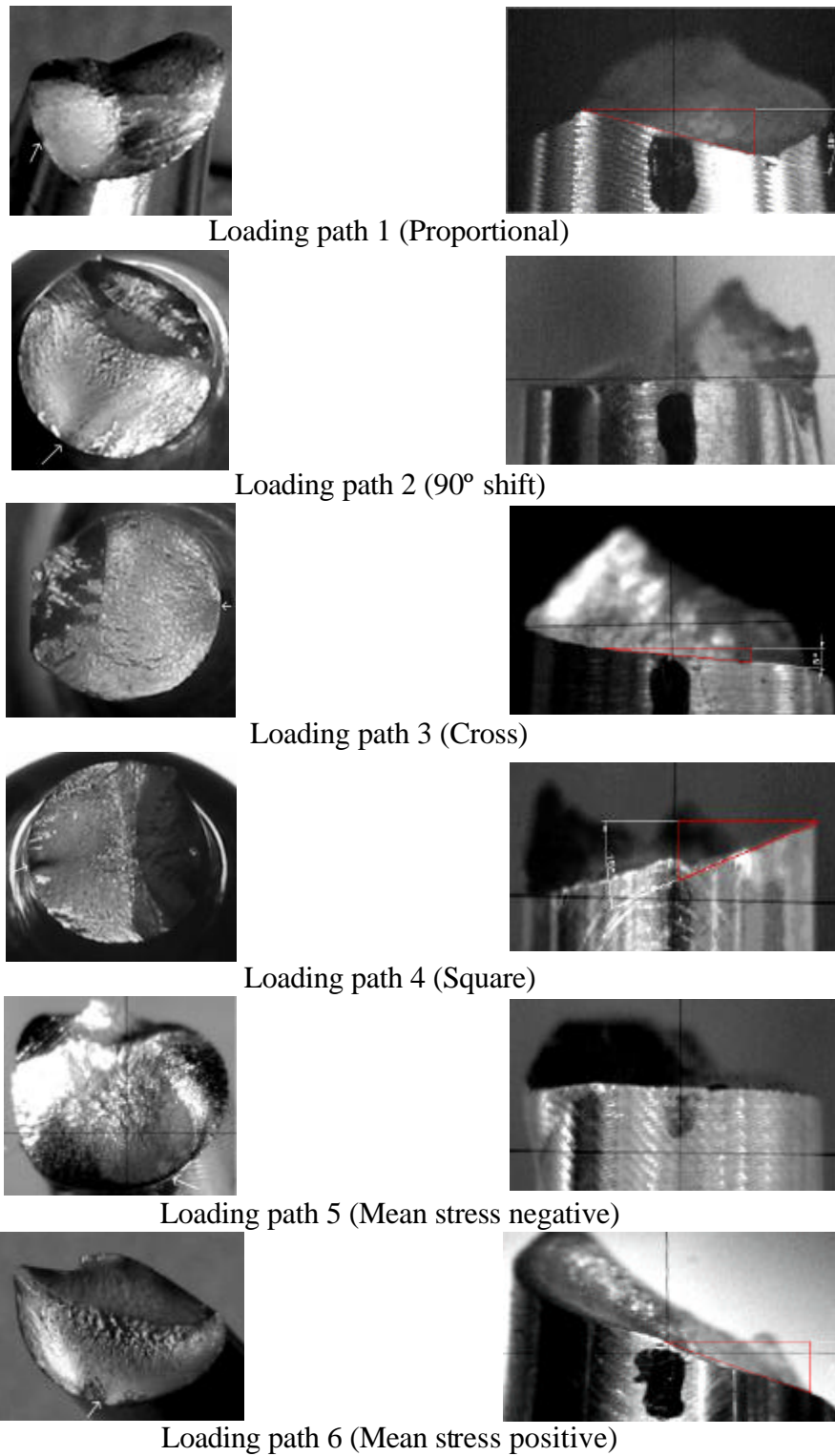


Figure 2. Fractographic analyses of the fatigue failure plane orientations under each of the six loading paths in Table 4.

## THEORETICAL ANALYSES OF THE FATIGUE CRACK PLANES

For the six biaxial loading cases shown in Table 4, the potential crack plane orientation is analysed by various critical plane models and energy-based critical plane model, such as the Findley, the Fatemi-Socie, the SWT and the Liu's criteria.

### *Findley Model*

Based on physical observations of the orientation of initial fatigue cracks in steel and aluminium, Findley [1] discussed the influence of normal stress acting on the maximum shear stress plane. A critical plane model was introduced, which predicts that the fatigue crack plane is the plane orientation  $\hat{e}$  with maximum Findley damage parameter:

$$\max_q (\tau_a + k \sigma_{n,\max}) \quad (1)$$

where  $\tau_a$  is the shear stress amplitude on a plane  $\hat{e}$ ,  $\sigma_{n,\max}$  is the maximum normal stress on that plane. Figure 3 shows the variations of the Findley parameter on the different plane  $\hat{e}$ , under the six loading cases. For each loading case, the plane angle with the maximum Findley parameter can be identified and they are summarized in Table 5.

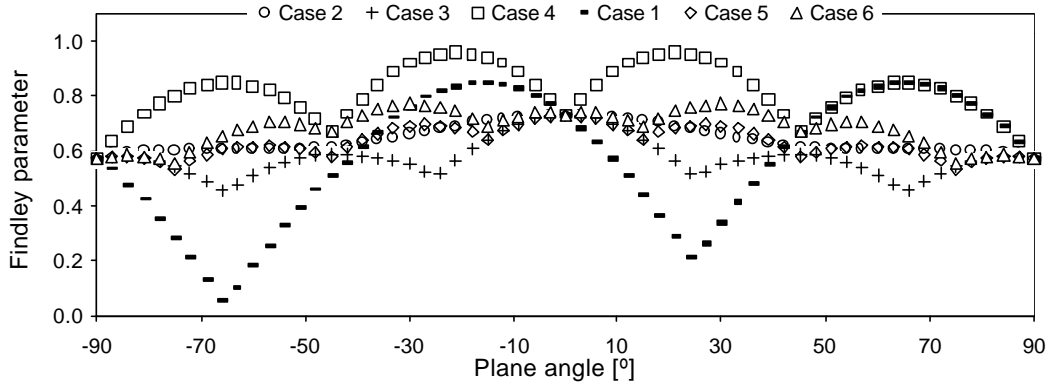


Figure 3. Variations of the Findley parameter on different plane.

### *Fatemi-Socie Model*

The Fatemi-Socie model [2] is widely applied for shear damage model, which predicts the critical plane is the plane orientation  $\hat{e}$  with the maximum F-S damage parameter:

$$\left[ \frac{\Delta \gamma}{2} \left( 1 + k \frac{\sigma_{n,\max}}{\sigma_y} \right) \right]_{\max_q} \quad (2)$$

where  $\Delta \gamma/2$  is the maximum shear strain amplitude on a plane  $\hat{e}$ ,  $\sigma_{n,\max}$  is the maximum normal stress on that plane,  $\sigma_y$  is the material monotonic yield strength;  $k$  is a material

constant, which can be found by fitting fatigue data from simple uniaxial tests to fatigue data from simple torsion tests.

Application of the Fatemi-Socie model for the six loading cases show the variations of the F-S parameter on different plane orientations as presented in Fig. 4. For each loading case, the plane angle  $\vartheta$  with the maximum F-S parameter can be identified and they are summarized in Table 5.

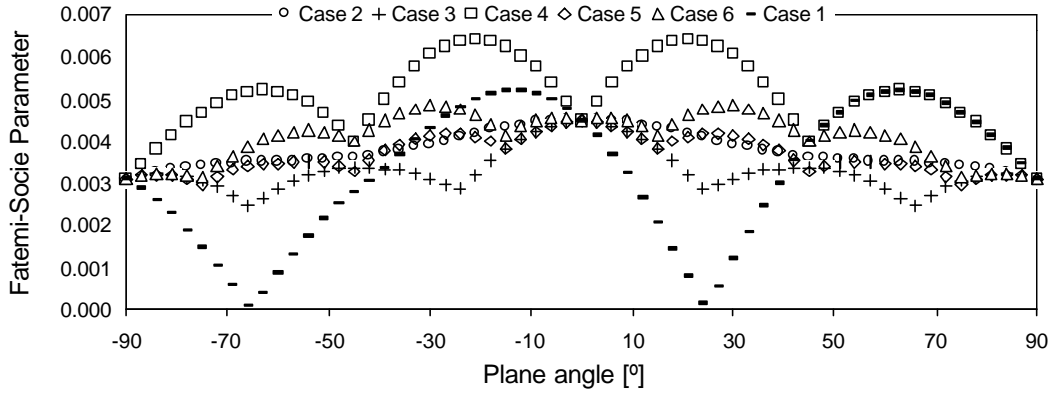


Figure 4. Variations of the F-S parameter on different plane.

### *S-W-T Model*

The tensile damage model, proposed by Smith, Watson and Topper [3], predicts that the fatigue crack plane is the plane orientation  $\vartheta$  with maximum normal stress (the maximum principal stress):

$$\max_q (\mathbf{s}_n) \frac{\mathbf{e}_1}{2} \quad (3)$$

where  $\sigma_n$  is the normal stress on a plane  $\vartheta$ ,  $\varepsilon_1$  is the normal strain on that plane.

Figure 5 shows the variations of the normal stress  $\sigma_n$  on the different plane  $\vartheta$ , under the six loading cases. For each loading case, the plane angle with the maximum normal stress  $\sigma_n$  can be identified and they are summarized in Table 5.

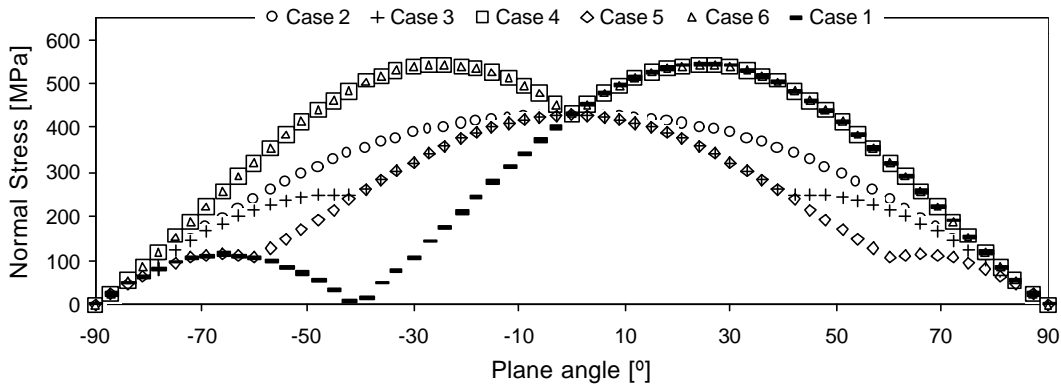


Figure 5. Variations of the normal stress  $\sigma_n$  on different plane.

### Liu's Virtual Strain-Energy Model

The Liu's virtual strain energy model [4] is an energy-based critical plane model. This model considers two possible failure modes: a mode for tensile failure,  $\Delta W_I$ , and a mode for shear failure,  $\Delta W_{II}$ . Failure is expected to occur on the plane  $\theta$  in the material having the maximum VSE quantity.  $\Delta W_I$  is computed by firstly identifying the plane on which the axial work is maximized and then adding the respective shear work on that same plane:

$$\Delta W_I = (\Delta \mathbf{s}_n \Delta \mathbf{e}_n)_{\max} + (\Delta t \Delta \mathbf{g})_q \quad (4)$$

Similarly,  $\Delta W_{II}$  is computed by firstly identifying the plane on which the shear work is maximized and then adding the axial work on that same plane:

$$\Delta W_{II} = (\Delta \mathbf{s}_n \Delta \mathbf{e}_n) + (\Delta t \Delta \mathbf{g})_{\max}_q \quad (5)$$

where  $\Delta \tau$  and  $\Delta \gamma$  are the shear stress range and shear strain range, respectively,  $\Delta \sigma_n$  and  $\Delta \epsilon_n$  are the normal stress range and normal strain range, respectively.

Application of the Liu's model for the six loading cases show the variations of the Virtual Strain Energy on different plane orientations as presented in Fig. 6 for  $\Delta W_I$  and Fig. 7 for  $\Delta W_{II}$ . For each loading case, the plane angle  $\theta$  with the maximum  $\Delta W_I$  and  $\Delta W_{II}$  parameters can be identified and they are summarized in Table 5.

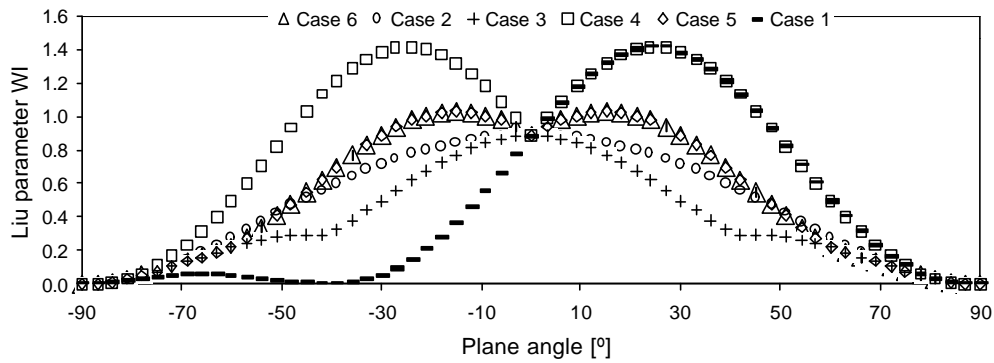


Figure 6. Variations of the Liu's  $\Delta W_I$  parameter on different plane.

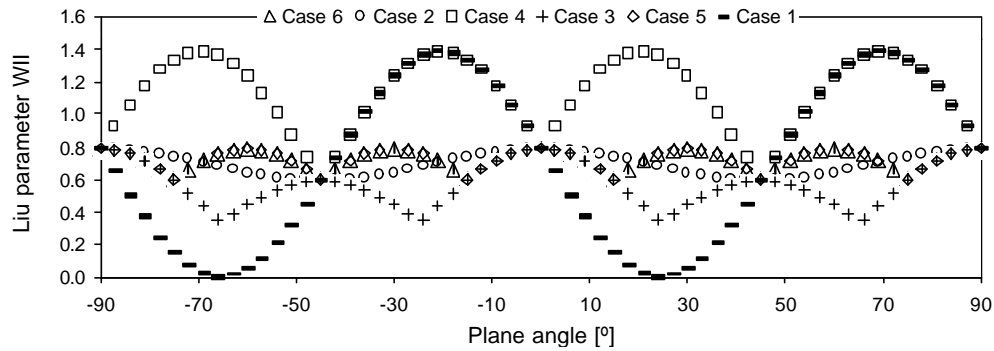


Figure 7. Variations of the Liu's  $\Delta W_{II}$  parameter on different plane.

## COMPARISONS BETWEEN EXPERIMENTS AND PREDICTIONS

The theoretical predictions of the crack orientations by the multiaxial fatigue models are compared with the experimental observations in Table 5. As can be observed from the table, in general, the shear-based models (Findley, Fatemi-Socie and Liu II) give better predictions than the tensile-based models (SWT and Liu I). From the shear-based models, Findley's criterion gives the best prediction, which the maximum deviation is 6°, in the square loading path.

Table 5. Comparison of the observed crack plane with predictions.

Loading Path	Crack Plane observed	Findley	Fatemi Socie	SWT	Liu I	Liu II
Case 1	-16°	-16° / 65°	-14° / 63°	26°	25°	-20°/70°
Case 2	0°	0°	0°	0°	0°	0°
Case 3	-5°	0°	0°	0°	0°	0°
Case 4	15°	±21°	±21°	±25°	±25°	±21°
Case 5	0°	0°	0°	0°	±15°	±30°/ 0°
Case 6	-28°	±29°	±29°	±25°	±15°	±30°/ 0°

## CONCLUSIONS

A wide range of fatigue loading paths were applied to a quenched and tempered alloy steel (42CrMo4). The initiation crack plane, observed by microscope, is influenced by the loading paths. For the studied material, the shear-based multiaxial models (Findley, Fatemi-Socie and Liu II) give very good predictions of the orientation of the crack initiation plane. The comparison between these shear-based models and the crack plane observed and measured were quite accurate.

## ACKNOWLEDGEMENTS

Financial support from the Fundação para Ciência e Tecnologia (FCT) is acknowledged.

## REFERENCES

1. Findley, W.N. (1959) *Journal of Engineering for Industry*, 301-306.
2. Fatemi, A. and Socie, D. (1988) *Fatigue and Fracture of Engineering Materials and Structures* **11**(3), 149-165.
3. Smith, R.N., Watson, P. and Topper, T.H. (1970) *J. of Materials* **5**(4), 767-778.
4. Liu, K.C. (1993) *Advances in Multiaxial Fatigue*. ASTM STP 1191, D.L. McDowell and R. Ellis, Eds, pp. 67-84.